

# Critical currents for vortex defect motion in superconducting arrays

Jong Soo Lim,<sup>1</sup> M.Y. Choi,<sup>1,2</sup> Beom Jun Kim,<sup>3</sup> and J. Choi<sup>4</sup>

<sup>1</sup>*Department of Physics, Seoul National University, Seoul 151-747, Korea*

<sup>2</sup>*Korea Institute for Advanced Study, Seoul 130-722, Korea.*

<sup>3</sup>*Department of Molecular Science and Technology, Ajou University, Suwon 442-749, Korea*

<sup>4</sup>*Department of Physics, Keimyung University, Daegu 704-701, Korea*

We study numerically the motion of vortices in two-dimensional arrays of resistively shunted Josephson junctions. An extra vortex is created in the ground states by introducing novel boundary conditions and made mobile by applying external currents. We then measure critical currents and the corresponding pinning energy barriers to vortex motion, which in the unfrustrated case agree well with previous theoretical and experimental findings. In the fully frustrated case our results also give good agreement with experimental ones, in sharp contrast with the existing theoretical prediction. A physical explanation is provided in relation with the vortex motion observed in simulations.

PACS numbers: 74.81.Fa, 74.25.Qt, 74.25.Sv

In equilibrium the two-dimensional Josephson junction array (JJA) is well known to exhibit the Berezinskii-Kosterlitz-Thouless transition,<sup>1</sup> which is driven by unbinding of vortex-antivortex pairs. Unbound vortices, while in motion, dissipate energy and thus make the system resistive. Without an external magnetic field this happens above the critical temperature. It is possible, however, to induce an unpaired vortex (defect) at low temperatures, e.g., by applying weak magnetic fields. Such a field-induced vortex defect sits on a plaquette where energy takes its local minimum; this is separated by the potential barrier set by the underlying lattice. The defect may be driven into motion by external currents, as it is exerted by the force  $\mathbf{F} = (h/2e)\mathbf{J} \times \hat{\mathbf{z}}$  with  $\mathbf{J}$  being the external current density on the  $xy$  plane. When the driving force is sufficiently strong, the defect can overcome the barrier to move onto the adjacent plaquette and accordingly give rise to non-vanishing voltage. Theoretical calculation of the barrier height is based on the iteration method, static in nature.<sup>2,3</sup> On the other hand, in experiment, the barrier height is determined dynamically, by measuring critical depinning currents.<sup>4</sup>

In the absence of background frustration  $f = 0$ , where  $f$  measures the number of flux quanta per plaquette, this barrier has been estimated as  $E_B(f=0) \approx 0.199$  in units of the Josephson coupling energy  $E_J$ .<sup>2,3</sup> The critical current in this case has been obtained from the onset of instability of the phase configuration and found to be  $I_c(f=0) \approx 0.105$  in units of the single-junction critical current  $i_c$ , which agrees well with experiment.<sup>4</sup> For high magnetic fields, say,  $f = 1/2$ , however, the numerically estimated value does not agree with the experimental one:  $E_B(1/2)/E_B(0) \approx 6$  for the former whereas  $E_B(1/2)/E_B(0) \approx 1.3$  for the latter. This discrepancy has remained unexplained since then.

This work is to bridge the gap between theory and experiment: We perform extensive dynamic simulations of the resistively-shunted junction (RSJ) model, which conveniently describes real dynamics of JJAs. Unlike existing studies, which were limited mostly to the defect-free case because of the difficulty to create a single defect

in the presence of external currents, we introduce novel boundary conditions for a single *extra* vortex and study its motion in the ground state of the  $f = 1/2$  system as well as the  $f = 0$  one. We then measure the critical current  $I_c$  and the corresponding energy barrier  $E_B$  to vortex defect motion; this is, to the best of our knowledge, the first direct numerical *measurement* of the barrier height. It is confirmed that our results for  $f = 0$  agree well with existing numerical and experimental values;<sup>4,5</sup> also revealed in the fully-frustrated ( $f = 1/2$ ) JJA is excellent agreement of our results with experimental ones unexplained so far. Via direct observation of actual vortex motion, we suggest that the previous overestimation of the energy barrier can be attributed to the unrealistic configuration of vortices.

We begin with an  $L \times L$  square array of RSJs between superconducting grains, with shunt resistance  $R$ . The  $i$ th grain, located at position  $\mathbf{r}_i$ , is described by its phase  $\{\phi_i\}$ . In order to compute the energy barrier, it is necessary to create just one extra vortex in the system. Both periodic boundary conditions (PBC) and fluctuating twist boundary conditions (FTBC),<sup>6</sup> used most frequently, allow  $f = n/L$  with an integer  $n$  and thus produce at the least  $L$  extra vortices. This problem can be remedied by using the diagonally antiperiodic boundary conditions (DAPBC) that introduce  $2\pi$  rotations of the phase variables around the whole system and thus produce a single extra vortex.<sup>7</sup> However, the straightforward application of DAPBC to dynamic simulations fails in the presence of external currents since the global current conservation cannot be fulfilled.<sup>6</sup> We thus modify FTBC in such a way that the system contains one additional vortex. In FTBC, the gauge-invariant phase difference is decomposed into two parts: One is periodic across the system and thus does not carry voltage whereas the other, called the fluctuating twist variable, is directly related to the voltage drop across the system. On the former part the boundary conditions of the DAPBC type, detailed in Ref. 8, are then imposed, relating only the boundary phase variables on the same columns and rows; this makes the application of the FTBC straightforward.

Equations of motion for the system (without capacitive and inductive couplings) then read, after scaling the time in units of  $\hbar/2ei_cR$ ,

$$\sum_j' \left[ \frac{d\tilde{\phi}_{ij}}{dt} + \sin(\tilde{\phi}_{ij} - \mathbf{r}_{ij} \cdot \Delta) \right] = 0, \quad (1)$$

where the primed summation runs over the nearest neighbors of grain  $i$ ,  $\mathbf{r}_{ij} \equiv \mathbf{r}_i - \mathbf{r}_j$  is a unit vector with the lattice constant set to unity, and  $\tilde{\phi}_{ij} \equiv \phi_i - \phi_j - A_{ij}$ , together with the voltage-carrying part, describes the gauge-invariant phase difference between sites  $i$  and  $j$ . The bond angle  $A_{ij}$ , given by the line integral of the vector potential, takes in the Landau gauge the values

$$A_{ij} = \begin{cases} 0 & \text{for } \mathbf{r}_j = \mathbf{r}_i + \hat{\mathbf{x}} \\ 2\pi f x_i & \text{for } \mathbf{r}_j = \mathbf{r}_i + \hat{\mathbf{y}} \end{cases}$$

with  $\mathbf{r}_i$  denoting the position of site  $i$ . The time evolution of the twist variable  $\Delta \equiv (\Delta_x, \Delta_y)$  is governed by<sup>6</sup>

$$\begin{aligned} \frac{d\Delta_x}{dt} &= \frac{1}{L^2} \sum_{\langle ij \rangle_x} \sin(\tilde{\phi}_{ij} - \Delta_x) - I_{dc} \\ \frac{d\Delta_y}{dt} &= \frac{1}{L^2} \sum_{\langle ij \rangle_y} \sin(\tilde{\phi}_{ij} - \Delta_y), \end{aligned} \quad (2)$$

where  $\sum_{\langle ij \rangle_a}$  denotes the summation over all nearest neighboring pairs in the  $a (= x, y)$  direction and the dc current  $I_{dc}$  (measured in units of  $i_c$ ) is injected along the  $x$  direction.

We use the second-order Euler algorithm to integrate Eqs. (1) and (2) with the time step of size  $\Delta t = 0.05$ . As initial conditions, we use the well-known ground-state phase configurations obtained with the conventional PBC: the ferromagnetic configuration  $\phi_i = 0$  for  $f = 0$  and the checker-board configuration  $\phi_{ij} = \pi/4$  for  $f = 1/2$ . After appropriate equilibration, the zero-temperature vortex configurations in Fig. 1 are obtained, which manifestly show the location of the extra vortex and justify the boundary conditions employed. We then apply the external dc current  $I_{dc}$  and measure the voltage drop (in units of  $i_c R$ )

$$\langle V \rangle = -\frac{\hbar L}{2e} \left\langle \frac{d\Delta_x}{dt} \right\rangle, \quad (3)$$

with  $\langle \dots \rangle$  denoting the time average and the energy

$$E = -\sum_{\langle ij \rangle} \cos(\tilde{\phi}_{ij} - \mathbf{r}_{ij} \cdot \Delta). \quad (4)$$

in units of the Josephson coupling strength  $E_J \equiv \hbar i_c / 2e$ . Typically, data for physical quantities have been averaged over  $5 \times 10^5$  time steps after equilibration over  $3 \times 10^4$  time steps for the JJA with size up to  $L = 120$ .

Figure 2 shows the current-voltage ( $IV$ ) characteristics for (a)  $f = 0$  and (b)  $f = 1/2$  in the system of size  $L =$

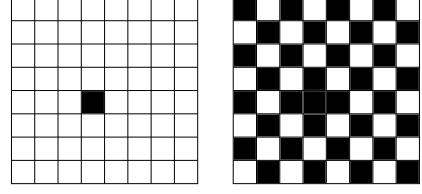


FIG. 1: Zero-temperature vortex configurations under the boundary conditions in Ref. 8 for  $f = 0$  (left) and  $f = 1/2$  (right). Filled squares denote the plaquettes occupied by vortices.

24, 32, and 64 (from top to bottom). It is observed that nonzero voltage drop develops as  $I_{dc}$  is increased beyond the critical current  $I_c$ , the size dependence of which are shown in the insets. As  $L \rightarrow \infty$ , the critical currents for defect motion unambiguously approach well-defined values from above<sup>9</sup> and the two-parameter least-square fits yield

$$\begin{aligned} I_c(f=0) &= 0.101(1) \\ I_c(f=1/2) &= 0.091(1), \end{aligned}$$

respectively, where the numbers in the parenthesis denote the numerical errors in the last digits. Our obtained value  $I_c(0)$  is essentially the same as the known value,<sup>4</sup> confirming the validity of our modified FTBC. For  $f = 1/2$ , however, our result sharply disagrees with the numerical value  $I_c(1/2) \approx 0.32$  in Ref. 4 and appears much smaller than that of the defect-free system.<sup>10</sup> This indicates that the critical current to make the point defect mobile is much less than the corresponding current for the rigid motion of the vortex superlattice. Remarkably, our results of the critical current are consistent with the experimental result  $I_c \approx 0.1$ , below which the dynamical resistance is negligible for any value of  $f$ .<sup>5</sup> It is to be noted here that our results are obtained from the direct numerical calculation of the  $IV$  characteristics while other studies present mostly indirect estimates from the pinning energy barrier with the phase configuration of given vorticities assumed (see below).<sup>4</sup>

Our simulations also allow us to directly measure the pinning energy barrier. To this end, we first plot in Fig. 3 the energy in Eq. (4) as a function of time in the array of size  $L = 120$  at the external current slightly higher than the critical value:  $I_{dc} = I_c(f, L) + 0.0001$ . Observed are oscillatory behaviors of  $E(t)$  in two very different time scales. While the long-period oscillations (only one period of which is shown for simplicity) describe the global motion of the defect, the small oscillations shown in insets disclose the defect motion in short length scales. The former arise from the defect motion across the system, i.e., the defect eventually arriving at one end of the system and then entering again from the other end. The lower energy values at both ends of the system reflect boundary effects, and the asymmetry in the behavior manifests

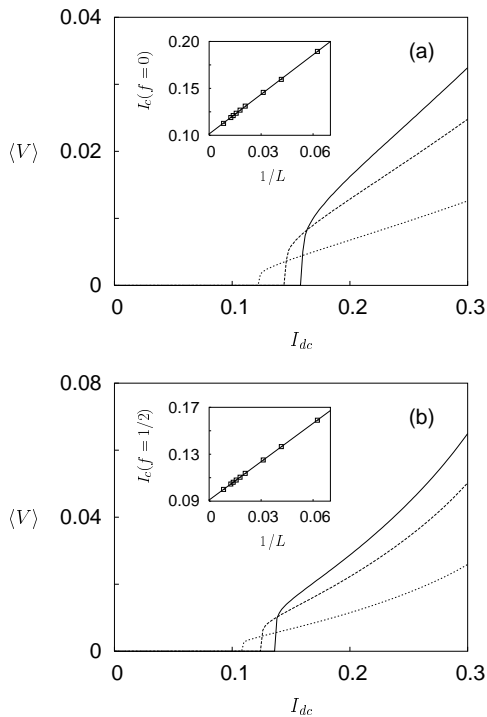


FIG. 2:  $IV$  characteristics at (a)  $f = 0$  and (b)  $f = 1/2$  for the system size  $L = 24, 32$ , and  $64$ , respectively, from top to bottom.  $I_{dc}$  and  $\langle V \rangle$  are expressed in units of  $i_c$  and  $i_c R$ , respectively. Insets show critical currents  $I_c$  as functions of the system size  $L$ .

that the symmetry of the potential energy around the middle of the system is broken by the driving currents.

On the other hand, the small oscillations in the insets are directly related with the lattice pinning effects. The local minimum (dip) of the energy corresponds to the (extra) vortex sitting down at the center of a plaquette whereas the peak is produced by the vortex on a link in the course of moving on to the adjacent plaquette. In the case of  $f = 0$ , there appears only one peak in a period. Since there are  $L$  lattice pinning barriers for a defect to move across the system, the longer oscillation in Fig. 3(a) consists of  $L$  small oscillations. For  $f = 1/2$ , although overall features are similar to those for  $f = 0$ , the shape of the pinning barrier is markedly different [see the inset of Fig. 3(b)]: One small oscillation consists of double peaks separated by a small dip and these peaks are separated by bigger dips. The number of bigger dips turns out to be  $L/2$ , which reveals that the defect motion for  $f = 1/2$  is periodic in space with the period twice the lattice constant; this reflects the  $2 \times 2$  translational symmetry of the vortex superlattice structure in the ground state. We define the pinning energy barrier  $E_B$  to be the energy difference between the bigger dip and the peak, neglecting the smaller one.

To minimize the boundary effects, we measure the barrier at the maximum of the long-period oscillation,

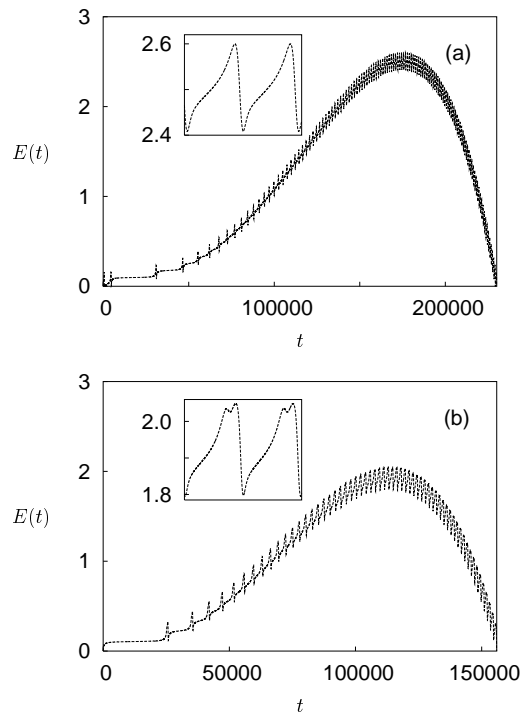


FIG. 3: Energy  $E(t)$  versus time  $t$  for (a)  $f = 0$  and (b)  $f = 1/2$  in the system of size  $L = 120$  at injected currents  $I_{dc} = 0.1128$  for  $f = 0$  and  $0.1001$  for  $f = 1/2$ . For convenience,  $E(t)$  has been shifted such that  $E = 0$  is the minimum. Insets display expansion plots of  $E(t)$  near maxima.

namely when the defect resides near the center of the system. Figure 4 presents the measured barrier height versus the system size. The extrapolation to the thermodynamic limit leads to<sup>11</sup>

$$\begin{aligned} E_B(f=0) &= 0.192(1) \\ E_B(f=1/2) &= 0.255(1). \end{aligned}$$

The resulting ratio,  $E_B(1/2)/E_B(0) \approx 1.33$ , is again in good agreement with the experimental result in Ref. 4. Note the dramatic improvement over the existing value,  $E_B(1/2)/E_B(0) \approx 6$ , obtained via the iteration method.

We now provide a physical explanation as to the origin of the previous discrepancy, in relation with the vortex motion directly observed in our simulations. We display in Fig. 5 the vortex motion in the  $f = 1/2$  background, which reveals the two-step process in the defect motion: The defect first pushes away the nearby vortex to make the plaquette vacant and subsequently occupies this vacancy. This type of motion gives rise to small oscillations of the energy in Fig. 3. In the numerical estimate in Ref. 4, however, the vortex defect was assumed to sit on the top of the other (background) vortex, which results in much higher energy due to strong on-site repulsion. This type of vortex configuration implies that the extra vortex moves in the rigid vortex lattice background, which is different from the actual motion of the

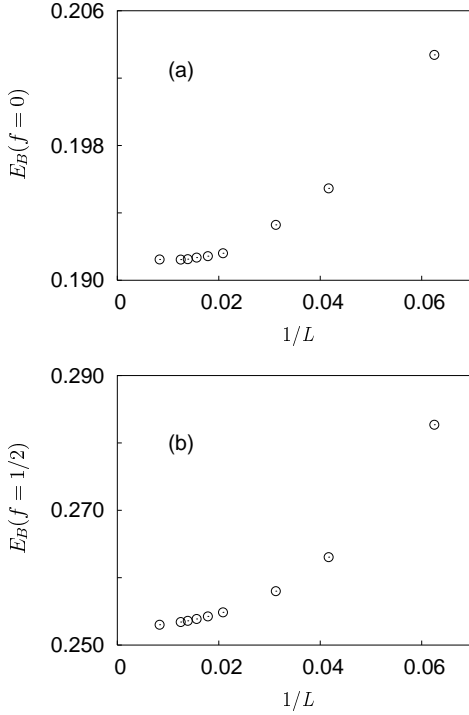


FIG. 4: Pinning barrier height  $E_B(f)$  as a function of the system size  $L$  for (a)  $f = 0$  and (b)  $f = 1/2$ . Systems of size up to  $L = 120$  are displayed.

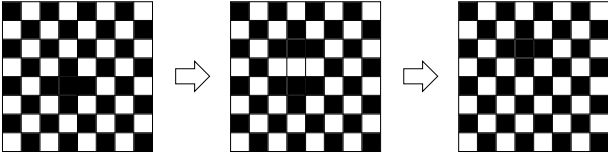


FIG. 5: Pattern of the defect motion in the system with  $f = 1/2$ . Currents are applied along the  $-x$  direction (i.e., from right to left).

vortices shown in Fig. 5. We believe that the latter type of actual motion occurs in experiment. Namely, vortex motion is influenced by background vortices present in the frustrated system, thus yielding substantially lower critical currents.

In summary, we have introduced novel boundary conditions which are convenient to study vortex dynamics in JJAs. From dynamic simulations in the presence of external currents and magnetic fields, the critical currents as well as the pinning energy barriers to vortex motion have been directly measured without any a priori assumption on the vortex configuration. For  $f = 0$ , our results agree fully with previous theoretical and experimental results. For  $f = 1/2$ , our results also give excellent agreement with experimental ones, in contrast with the previous theoretical prediction. From the direct observation of the vortex motion, it has been found that for  $f = 1/2$  the defect moves in the two-step process with two vortices involved, producing double peaks in the energy barrier. This suggests that vortices move interactively when a large number of vortices are present.

This work was supported in part by the KOSEF Grant R01-2002-000-00285 and the SKOREA program (JSL, MYC) and by the KRF Grant 2003-041-C00137 (BJK).

<sup>1</sup> For a list of references, see, e.g., *KT Transitions and Superconducting Arrays*, edited by D. Kim, J.S. Chung, and M.Y. Choi (Min Eum Sa, Seoul, 1993); *Macroscopic Quantum Phenomena and Coherence in Superconducting Networks*, edited by C. Giovannella and M. Tinkham (World Scientific, Singapore, 1995).

<sup>2</sup> C.J. Lobb, D.W. Abraham, and M. Tinkham, Phys. Rev. B **27**, 150 (1983).

<sup>3</sup> M. Yoon, M.Y. Choi, and B.J. Kim, Phys. Rev. B **61**, 3263 (2000).

<sup>4</sup> M.S. Rzchowski, S.P. Benz, M. Tinkham, and C.J. Lobb, Phys. Rev. B **42**, 2041 (1990).

<sup>5</sup> S.P. Benz, M.S. Rzchowski, M. Tinkham, and C.J. Lobb, Phys. Rev. B **42**, 6165 (1990).

<sup>6</sup> B.J. Kim, P. Minnhagen, and P. Olsson, Phys. Rev. B **59**, 11506 (1999).

<sup>7</sup> H. Kawamura and M. Kikuchi, Phys. Rev. B **47**, 1134(R) (1993).

(1993).

<sup>8</sup> The detailed boundary conditions on the phase variable  $\phi_{x,y}$  at position  $\mathbf{r} = (x, y)$  read

$$\begin{aligned} \phi_{0,1} &= \phi_{L,1} + 3\pi/2, & \phi_{L,0} &= \phi_{L,L} + 3\pi/2, \\ \phi_{L+1,L} &= \phi_{1,L} + 3\pi/2, & \phi_{1,L+1} &= \phi_{1,1} + 3\pi/2, \\ \phi_{0,y} &= \phi_{L,y} + \frac{3}{2}\pi - \frac{y-2}{L-1}\pi & \text{for } 2 \leq y \leq L, \\ \phi_{x,0} &= \phi_{x,L} + \frac{\pi}{2} + \frac{x-1}{L-1}\pi & \text{for } 1 \leq x \leq L-1, \\ \phi_{L+1,y} &= \phi_{1,y} + \frac{\pi}{2} + \frac{y-1}{L-1}\pi & \text{for } 1 \leq y \leq L-1, \\ \phi_{x,L+1} &= \phi_{x,1} + \frac{3}{2}\pi - \frac{x-2}{L-1}\pi & \text{for } 2 \leq x \leq L. \end{aligned}$$

<sup>9</sup> Note that under open boundary conditions the finite-size effects appear in the opposite way that larger systems are

less resistive. See M.Y. Choi, G.S. Jeon, and M. Yoon, Phys. Rev. B **62**, 5357 (2000). This is in parallel to the static Monte Carlo results where opposite size dependences have been observed under different boundary conditions. See, e.g., P. Olsson, Phys. Rev. Lett. **73**, 3339 (1994).

<sup>10</sup> B.J. Kim and P. Minnhagen, Phys. Rev. B **61**, 7017 (2000) and references therein.

<sup>11</sup> Consideration of the finite screening length, about 15 lattice spacings in the array in Ref. 4, results in a small change of the barrier height and does not change the conclusion. See J.R. Phillips, H.S.J. van der Zant, J. White, and T.P. Orlando, Phys. Rev. B **47**, 5219 (1993).